

NEW EXPERIMENTAL METHOD FOR INVESTIGATION OF THE NUCLEON POLARIZABILITIES

G.D. Alkhazov, V.P. Chizhov, E.M. Maev, E.M. Orischin, G.E. Petrov,
V.V. Sarantsev, Yu.V. Smirenin

1. Introduction

The electric α and magnetic β polarizabilities are basic structure constants of the nucleon, which characterize the response of the internal nucleon structure to the action of external electric and magnetic fields. The knowledge of α and β provides a stringent test of models describing the quark-meson structure of the nucleon, *e.g.*, in Chiral Perturbation Theory [1]. These polarizabilities are found by measuring Compton scattering cross-sections as a function of the photon energy and scattering angle and by a best fit using a theoretical description with the quantities of interest as open parameters. Experiments focus on photon energies below the pion mass because at these energies the Compton scattering cross-sections can be related model-independently to the polarizabilities through a Low Energy Theorem [2], which takes into account the proton structure in lowest order and shows that the scattering amplitude of Compton scattering off a system with spin $\frac{1}{2}$ can be expanded in powers of E_γ .

Recent experiments on Compton scattering to measure the polarizability of the proton and the deuteron were mostly performed using quasi-monoenergetic photons from bremsstrahlung tagging (see review of Shumacher [3]). The photons were scattered on liquid hydrogen or deuterium, and the scattered photons were detected under one or several scattering angles with NaI or BaF₂ spectrometers. These experiments provided the four-vectors p_i and the numbers of the incoming and scattered photons. A disadvantage of this method is a limited photon flux a tagger system can provide. To increase the luminosity, thick liquid targets were used.

In contrast to the above experiments, in the method proposed in [4] and developed at the Superconducting Darmstadt Electron Accelerator S-DALINAC, bremsstrahlung photons produced by an electron beam are used, and not only the angle and energy of the scattered photons but also the angle and energy of the recoiling protons (deuterons) are measured. This approach (sketched in Fig. 1) increases the luminosity and lowers the background considerably, especially below 50 MeV.

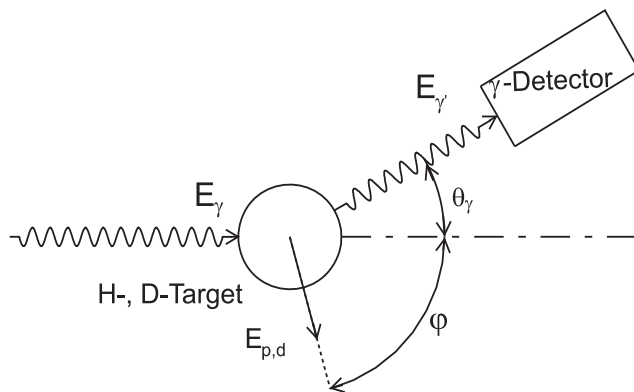


Fig. 1. Experimental method (schematic). A photon beam with a full bremsstrahlung spectrum is scattered from a gaseous hydrogen/deuterium target inside a high pressure ionization chamber, the energy of the scattered photons is determined in a γ -detector under a certain angle. By detecting the scattered bremsstrahlung photon in coincidence with the recoiling proton (deuteron) in the ionization chamber the incoming photon energy is determined

In this report, we describe the new method and a new experimental set-up for measuring the nucleon polarizabilities, and the performed test experiments. The photons scattered off protons in the ionization chambers are detected under two angles, 90° and 130° , by means of 10×14 in² NaI(Tl) detectors. The energies of the scattered photons are measured with the NaI(Tl) detectors, while the energies of the scattered recoil protons are measured with the ionization chambers (ICs), which serve simultaneously as targets and detectors.

2. Bremsstrahlung photon facility

A high-energy bremsstrahlung photon facility was built at the S-DALINAC [5]. The aim was to generate a high-intensity, nearly background-free photon beam. In this facility, a fully controlled electron beam is transformed into a photon beam by passing through a 0.3 mm thick (corresponding to 0.1 radiation lengths) bremsstrahlung-radiator made of gold. After the passage through two lead collimation systems into a 3 m concrete wall, the photon beam enters the experimental hall, where the Compton scattering set-up is installed. The position and intensity of the photon beam is measured downstream from the experiment by means of two special ionization chambers placed inside a hole in a concrete wall directly in front of the γ -beam stop for background minimization. The first chamber has segmented anode and cathode plates and allows an online determination of the photon beam position. In future experiments, the position of the electron beam on the radiator target, and therefore the position of the photon beam will be steered with the help of the output signals of this detector. The second ionization chamber is the so called Gaussian quantameter [6]. It allows to measure the γ integrated beam power in a wide energy range from 10 MeV up to several GeV.

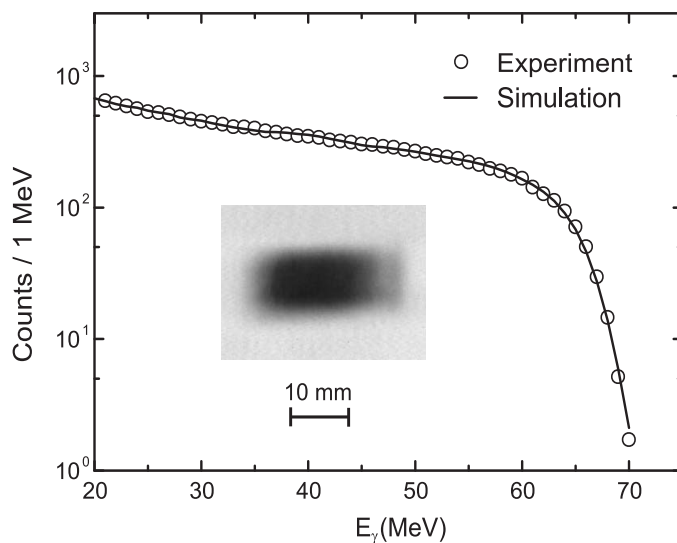


Fig. 2. Bremsstrahlung spectra and a part of a colour inverted Polaroid picture of the collimated bremsstrahlung beam approximately 3 m behind the bremsstrahlung target: Areas with high beam intensity are dark, with low intensity are grey. Circles correspond to the measured bremsstrahlung spectrum. The curve shows a folded simulation spectrum

In order to determine the absolute cross-sections for the Compton scattering off the proton (deuteron) with the reported technique, it is essential to know not only the integral intensity of the photon beam measured with the above-mentioned quantameter, but also the shape of the energy spectrum of the beam. The shape of this spectrum is determined with two additional $10 \times 10 \text{ in}^2$ NaI-spectrometers, which detect Compton scattered photons from the atomic electrons in the exit beryllium window of the ionization chambers. They are placed approximately 10 m downstream from this window under angles of 1.89° and 2.42° , respectively. Photons Compton scattered from electrons under these angles have the same energies as photons Compton scattered off the proton in the ionization chambers at 90° and 130° . The $10 \times 10 \text{ in}^2$ spectrometers are equipped with the same active and passive shielding as the main γ -spectrometers. With the knowledge of the response functions of the NaI(Tl) crystals it is possible to evaluate the intensity as well as the shape of the energy spectrum of the incoming bremsstrahlung beam. Figure 2 shows the energy spectrum of the bremsstrahlung beam measured with the above-mentioned γ -spectrometer in comparison with the results of GEANT4 calculations. Excellent agreement is observed. A colour-inverted Polaroid picture of the collimated γ -beam cross-section obtained 3 m behind the bremsstrahlung target is also shown as insert in this figure. The beam spot size at this position corresponds to a size of $20 \times 10 \text{ mm}^2$ inside the ICs.

3. γ -ray spectrometers

All NaI(Tl) photon spectrometers for detecting the scattered photons are items on loan from the Institute of Nuclear Physics of the Johannes Gutenberg-Universität, Mainz. Those used to detect the photons scattered from protons (deuterons) are $10 \times 14 \text{ in}^2$ in size. Compton scattered photons from the ionization chambers enter these γ -spectrometers through collimation systems, which determine a solid angle of about 10 msr. With this collimator system only the inner part of the γ -detectors is hit, which reduces the low-energy tails in the response functions. An energy calibration was achieved up to $E_\gamma = 4.44 \text{ MeV}$ with the help of standard γ -sources. At higher energies, the energy calibration was performed by using an electron beam with the known energy, and detecting electrons scattered from an aluminum target replacing the hydrogen ionization chamber. According to GEANT4 simulations, the response functions of the detectors for photons and electrons are practically identical. An extrapolation of the energy calibration parameters to the low-energy region shows good agreement with the results of the γ -source measurements. Since these detectors work as trigger detectors and the dead time of the ionization chamber is rather long (about $4 \mu\text{s}$), it is essential to minimize their background counting rate. Therefore, the NaI(Tl) crystals are well shielded.

4. High pressure ionization chambers

The detector of recoil protons (deuterons) consists of two ionization chambers combined in one volume. The incident photons scattered on the filling gas of the first (second) chamber are detected under the angle of 90° (130°). Both chambers have a cathode, a grid and an anode divided in strips (Fig. 3).

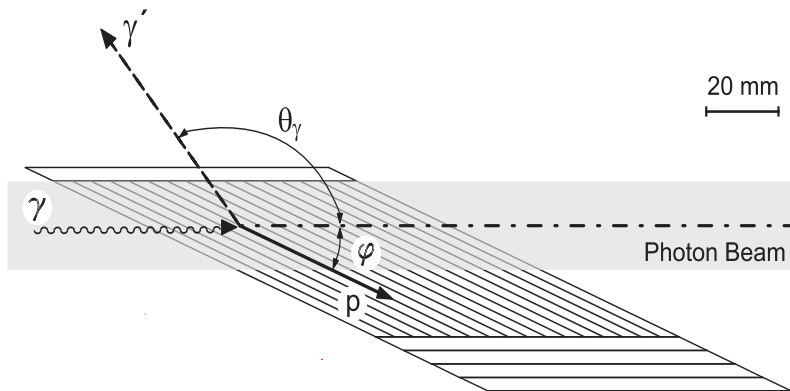


Fig. 3. Top view on a multi-strip anode: the 2 cm broad photon beam enters the volume of the IC from the left side. In the case a photon is scattered under the angle $\theta = 130^\circ$, the scattered proton gets a momentum along an anode strip (at $\phi = 22^\circ$)

The body of the chamber is made of stainless steel with a wall thickness of 14 mm. The photon beam enters (leaves) the chambers through 6 mm (7 mm) beryllium windows. This material was chosen in order to minimize the absorption of photons and production of e^+e^- -pairs. The Compton scattered photons on hydrogen at these selected angles ($\theta_\gamma = 90^\circ \pm 4^\circ$ and $\theta_\gamma = 130^\circ \pm 3^\circ$) leave the IC's through 9 mm beryllium windows to the γ -spectrometers. The ICs operate in the electron collection mode, *i.e.* the signals result from the electrons collected after ionization produced by protons. The applied high voltages are -40 kV on the cathode and -3.5 kV on the grid, the anode being at zero potential. The electron drift times are 3.5 and $0.12 \mu\text{s}$ for the cathode-grid and grid-anode distances, respectively. To select the recoiling proton, a special geometry of the IC anode is used. It is designed to detect tracks of recoiling protons in a background of tracks of Compton scattered electrons and secondary electron-positron pairs. The anode of the IC consists of several strips aligned along the direction of the recoil protons. In particular, in the case of Compton scattering under $\theta = 130^\circ$, the proton recoil angle ϕ is 22° . Along its path, the proton ionizes hydrogen molecules. As schematically shown in Fig. 4a, ionization electrons drift towards the anode and are collected there on one or two anode strips. When Compton scattered electrons and electron-positron pairs are formed, they have angles different from that of the recoil protons. The charges released by them are collected by several strips and produce only small signals on a single strip. In Fig. 4b, different simulated proton pulse forms are shown. At an azimuthal angle 0° (the proton track is parallel to the anode), the pulse lengths have a

minimal value and are equal for all energies. For protons with higher energies and at larger azimuthal angles, the pulse shape becomes wider and asymmetric.

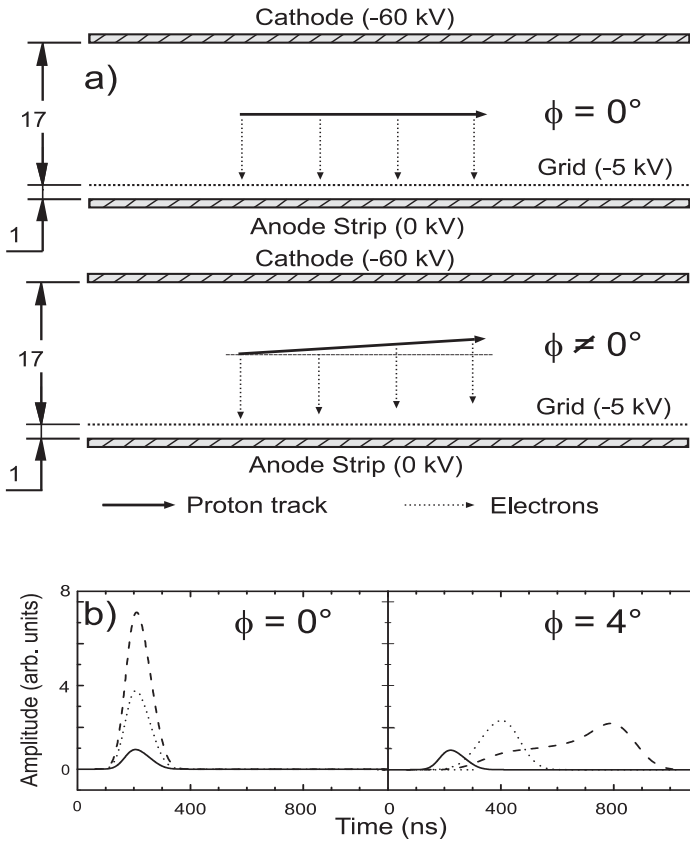


Fig. 4. a – side view of the chamber electrodes. The upper part shows a track of a proton, parallel to the anode. The lower part demonstrates a track of a proton under a finite angle. Dimensions are in mm; b – simulated pulse form for different azimuthal angles and for different proton energies: 1 MeV (solid line), 4 MeV (dotted line) and 8 MeV (dashed line)

Due to high hydrogen pressure in the ICs (75 bar), the effect of recombination of the electrons and positive ions formed by an ionizing particle becomes significant. The effect of recombination was studied for α -particles with a ^{237}Pu source ($E_\alpha = 5.15$ MeV) mounted on the IC cathodes. It was found to be rather large, reducing the registered signals by about 30 %. The effect of recombination in case of ionizing protons is expected to be noticeably smaller. According to [7], the collected charge produced by protons with energies $E_p \geq 0.5$ MeV in hydrogen at the conditions of our experiment can be estimated by the following empirical formula: $Q = e K (E_p - E') / W$, where $E' = 0.15$ MeV, $K = 0.9$, e is the electron charge, and $W = 36.3$ eV is the energy for electron-ion pair production in hydrogen. The proton recoil energy is thus

$$E_p = E' + QW / eK. \quad (1)$$

Another process that might cause a reduction of the registered signals is the attachment of electrons to electronegative impurities (such as O_2 and H_2O) in the working gas of the chambers. To reduce the amount of gas impurities, the chambers were heat trained under vacuum pumping. The hydrogen used for experiments contained less than 1 ppm impurities. Signals from a ^{237}Pu α -source were used for checking the gas quality. During the test experiments, the position of the energy peak of the 5.15 MeV α -particles decreased by $\sim 5\%$ per week, indicating slow evaporation of contaminants from the chamber walls. As simulations have shown, a noticeable amount of electrons (on the level of 0.1 %) appears in the photon beam in the active regions of the ionization chambers due to interaction of photons with the working gas of the chambers. To exclude registration of scattered electrons in the γ -ray spectrometers, anticoincidence scintillation counters, the so-called veto detectors, were placed in front of the NaI detectors.

5. Electronics

The electronics used in the data acquisition consisted mostly of standard NIM, CAMAC and VME components. The signals on the anodes of the ICs were registered by special low-noise preamplifiers, amplifier-discriminators and 14-bit 100 MHz Flash ADCs (FADCs). The FADCs digitize the analog signal in 10 ns steps continuously and hold the values for 4.5 μ s in a ring buffer memory. This is necessary, since the signals from ICs are delayed relative to the trigger pulse of the NaI(Tl) detectors by the drift time of electrons produced by recoil protons in the Compton scattering event. The trigger signals define a time window of 4.5 μ s, in which the proton pulse is expected to take place. The current on the IC anodes is always recorded within this window by the FADCs when a trigger signal is generated. Figure 5 shows an example of a recoil proton signal, registered by a FADC, in comparison with a GEANT4 simulation. The results of the measurement and the simulation are in good agreement.

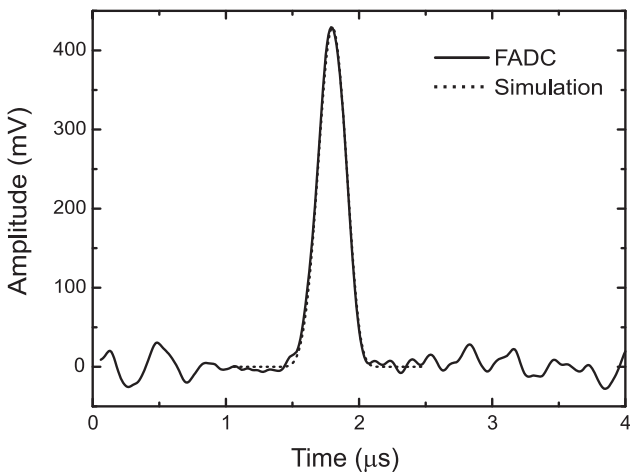


Fig. 5. Example of a signal in the IC from a 4 MeV recoil proton, registered by a FADC, compared to a GEANT4 simulation

The channels of the FADC have to be read out for each IC, which takes quite a long time (about several μ s) making it necessary to minimize the trigger rate. In order to improve the signal-to-noise ratio, the registered signals can be treated off-line with digital filters. A preliminary energy calibration of the amplifier channels was performed by inserting calibrated charges through a small capacitance to the anodes of the ICs. The NaI(Tl) detectors, which act as trigger detectors, are operated in anticoincidence mode with the surrounding plastic detectors. The signal is split in two: one signal starts the whole readout from the trigger module, the second signal is delayed by 4.5 μ s and stops the recording of the FADCs, which are then read out. This trigger unit also starts the readout of the ADCs, which digitize the NaI(Tl) energy pulses. In addition to the energy signals from the main γ -detectors (for registering γp -scattering) and the pulses on the anode strips of the ICs, data of other detectors like the quantameter, the position detectors, the Faraday cup and the signals from the γ -detectors for the beam monitoring are continuously read out and written onto tape or disk using the MBS data acquisition system.

6. Test experiments

Test experiments were performed at the S-DALINAC using bremsstrahlung photon beams with endpoint energies of 60 and 79.3 MeV. Electron beam currents ranged from 1 to 5 μ A. The ICs were filled with hydrogen gas of high purity (99.9999 %) at a pressure of 75 bar. The gas pressure was measured with a precision of about 0.5 %. In these test experiments about 5000 Compton scattered events in total were collected in coincidence with recoil protons. Figure 6 shows a typical drift-time distribution of signals which appeared at the IC anodes. This distribution reflects the γp -interaction points in the vertical direction. The width of this distribution corresponds to a vertical photon beam size of about 1 cm. It is seen that the position of the photon beam was not in the middle of the gap between the IC grid and the cathode, but closer to the grid. The number of events in the drift time interval from 2.5 to 3.5 μ s is small demonstrating that

the coincidence between the signals from the γ -spectrometers and the ionization chambers suppresses the background very efficiently. At the same time, one can see some events in the drift time interval of 0–0.5 μ s and 2–2.5 μ s. Presumably, these events appear due to some halo of the photon beam.

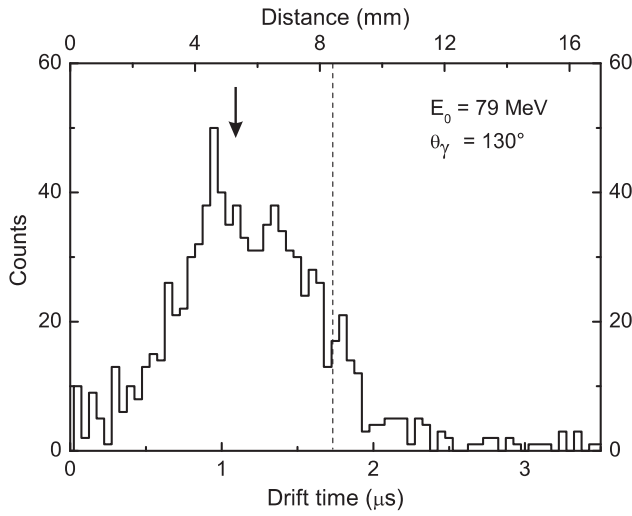


Fig. 6. Drift-time distribution of proton signals in an IC. The dashed line denotes the centre of the active volume between electrodes. The actual location of the photon beam is indicated by the arrow

The measured energy correlation between the scattered photons and recoiled protons is shown in Fig. 7 for the data taken at $E_0 = 60$ MeV, $\theta_\gamma = 130^\circ$ and energies $E_\gamma > 20$ MeV, $E_p > 1$ MeV. The experimental data are in good agreement with the expected kinematical relation. This figure also demonstrates that the background is rather small. Events on the left side of the (E_γ, E_p) correlation curve are partly due to tails of the γ -response function and partly due to background, which may be reduced in the future by building additional shielding for the γ -spectrometers.

The cross sections obtained in the experiments at $E_0 = 60$ and 79.3 MeV are shown in Fig. 8. The overall normalization of the (γ, p) cross sections measured as a function of the photon energy was performed with the help of the theoretical curve with $\alpha = 11.8$, $\beta = 2$ (dashed line). The resulting cross sections are in good agreement with a previous measurement [8] at comparable photon energies.

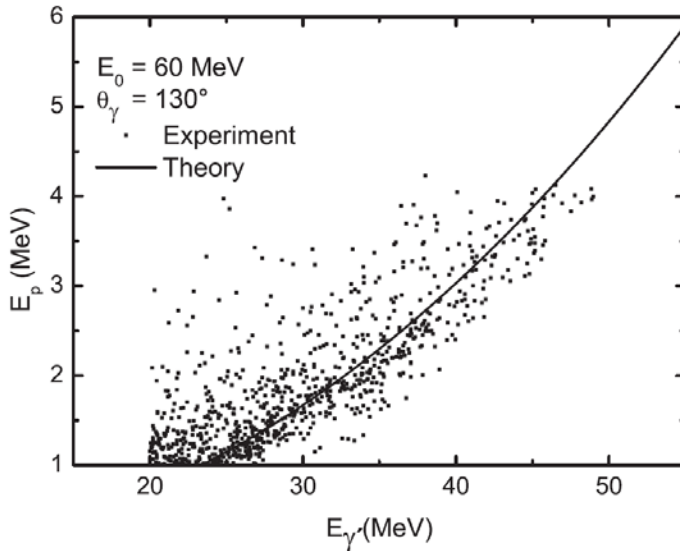


Fig. 7. Measured energy correlation of the scattered photons ($E_\gamma > 20$ MeV) and recoil protons ($E_p > 1$ MeV) in comparison with the expected kinematic relation for E_γ and E_p (solid curve) for the data taken at $E_0 = 60$ MeV and $\theta = 130^\circ$. The proton recoil energies are determined from the measured charges, collected on the IC anodes, with the help of Eq. (1)

Of course, the low statistics collected in the test experiment is not sufficient to extract meaningful results on the proton polarizabilities. From those measured values and the range of results from theoretical calculations [2] it has been estimated that in order to determine the values of α and β for the proton with a precision of $\Delta\alpha = 0.3$ and $\Delta\beta = 0.4$ with this technique it is necessary to perform measurements at a 100 MeV

electron beam (to increase the photon flux per incident electron) with an integrated beam current of $2.5 \times 10^4 \mu\text{Axh}$. The proposed new experimental method and the results of two test runs have shown that future high-statistics experiments to determine α and β are indeed feasible.

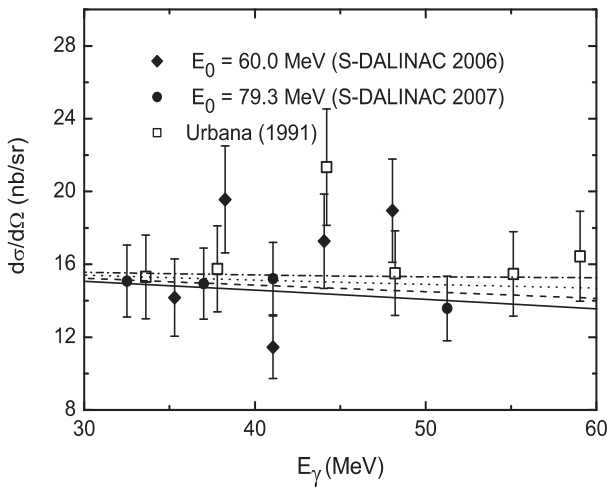


Fig. 8. Differential cross sections for Compton scattering on the proton obtained in the experiments at the S-DALINAC at $E_0 = 60$ MeV (full diamonds) and $E_0 = 79.3$ MeV (full circles) at an angle $\theta = 130^\circ$. Data from [8] in the same energy region and at an angle of 135° are given as squares. The lines correspond to calculations for different values of α and β : $\alpha = 13.8$, $\beta = 0$ (solid line), $\alpha = 11.8$, $\beta = 2$ (dashed line), $\alpha = 9.8$, $\beta = 4$ (dotted line), $\alpha = 7.8$, $\beta = 6$ (dashed-dotted line). The error bars include statistical contributions only. The data from the S-DALINAC are normalized with the theoretical curve shown as dashed line

7. Conclusion

A new method for measurements of the electric and magnetic polarizabilities (α and β) of the proton and deuteron has been proposed and tested. The new approach for determination of α and β is based on Compton scattering of untagged bremsstrahlung photons and registration of the recoil protons (deuterons) with special high-pressure hydrogen ionization chambers, which serve as targets and detectors. The scattered photons are registered with NaI(Tl) spectrometers. Test experiments have shown that the whole set-up functions in the expected way. The new experimental set-up for measuring the electric and magnetic nucleon polarizabilities is described in more detail in [5].

This work was performed in collaboration with O. Yevetska, S. Watzlavik, P. von Neumann-Cosel, J.-M. Porté, A. Richter, and G. Schrieder (Institut für Kernphysik, Technical University Darmstadt, Germany).

References

1. V. Bernard, N. Kaiser, U.-G. Meissner, *Int. J. Mod. Phys. E* **4**, 193 (1995).
2. A.I. L'vov, V.A. Petrun'kin, M. Schumacher, *Phys. Rev. C* **55**, 359 (1997).
3. M. Schumacher, *Prog. Part. Nucl. Phys.* **55**, 567 (2005).
4. D.V. Balin, M.J. Borkowski, V.P. Chizhov, G.A. Kolomensky, E.M. Maev, D.M. Seliverstov, G.G. Semenchuk, Yu.V. Smirenin, A.A. Vasiliev, A.A. Vorobyov, N.Yu. Zaitsev, Preprint PNPI-2104, Gatchina (1996).
5. O. Yevetska *et al.*, *Nucl. Instr. and Meth. A* **618**, 160 (2010).
6. A.P. Komar, S.P. Kruglov, I.V. Lopatin, *Nucl. Instr. Meth.* **82**, 125 (1970).
7. V.A. Volchenkov, E.M. Maev, V.P. Maleev, G.A. Ryabov, G.G. Semenchuk, Preprint PNPI-1368, Gatchina (1988).
8. F.J. Federspiel, R.A. Eisenstein, M.A. Lucas, B.E. MacGibbon, K. Mellendorf, A.M. Nathan, A. O'Neill, D.P. Wells, *Phys. Rev. Lett.* **67**, 1511 (1991).